Deep Radio Continuum Imaging of Dwarf Irregular IC 10: Tracing Star Formation And Magnetic Fields

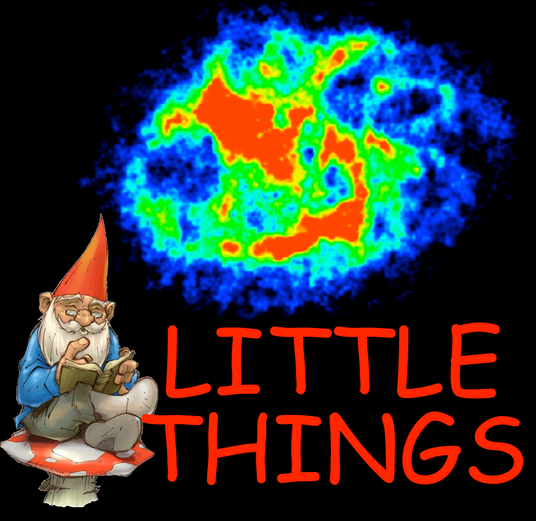

Volker Heesen[1], U. Rau[2], M. Rupen[2], E. Brinks[1], D. Hunter[3]

[1]University of Hertfordshire, United Kingdom, [2]NRAO, [3]Lowell Observatory

ABSTRACT

We exploit the vastly increased sensitivity of the Expanded Very Large Array (EVLA) to study the radio continuum and polarization properties of the post-starburst, dwarf irregular galaxy IC10 at 6 cm, at a linear resolution of ~50 pc. We find close agreement between radio continuum and Ha emission, from the brightest HII regions to the weaker emission in the disk. A quantitative analysis shows a strictly linear correlation, where the thermal component contributes 50% to the total radio emission, the remainder being due to a non-thermal component with a surprisingly steep radio spectral index of between -0.7 and -1.0 suggesting substantial radiation losses of the cosmic-ray electrons. We confirm and clearly resolve polarized emission at the 10-20% level associated with a non-thermal superbubble, where the ordered magnetic field is possibly enhanced due to the compression of the expanding bubble. A fraction of the cosmic-ray electrons has likely escaped because the measured radio emission is a factor of 3 lower than what is suggested by the Ha inferred SFR.

Introduction

Dwarf galaxies are the most abundant type of galaxy in the local universe and are the closest analogues to the building blocks for galaxy formation at high redshift in ΛCDM models. Furthermore, in the "downsizing" paradigm dwarf galaxies increasingly dominate the star-forming universe over time, with star formation (SF) perhaps being particularly enhanced within dwarfs over the past 2 Gyr. Stellar winds and supernova explosions of the most massive stars can easily lead to outflows due to their weak gravitational potential. This implies that not only does the metallicity of the interstellar medium (ISM) increase with cosmic time, but additionally the intergalactic medium becomes enriched at an early stage. Moreover, dwarf galaxies are supposed to have played a fundamental role in amplifying magnetic fields in the early universe through outflowing plasma escaping from star-forming regions (Chyzy et al. 2011, A&A, 529, 94).

Cosmic rays play an important role in galactic outflows, as they consist of relativistic particles that do not quickly lose their energy, like the hot gas. They spiral along magnetic field lines emitting highly linearly polarized, non-thermal (synchrotron) emission providing a useful tool to study magnetic field structure.

With the new capabilities of the Expanded Very Large Array (EVLA) and much improved sensitivity we can study the weak extended emission in dwarf galaxies. Here, we summarise first results from observations of IC 10 with the EVLA at C-band, which were published in the EVLA special edition of ApJ Letters (Heesen et al. 2011, ApJ, 739, L23).

Observations

We observed IC 10 with the NRAO EVLA under the resident shared risk program (RSRO) in D-configuration. We used a total bandwidth of 2 GHz between 4.5-5.4GHz and 6.9-7.8GHz, respectively. We calibrated the data with the Common Astronomy Software Applications package (CASA). We performed one round of amplitude and phase self-calibration, and the resulting image achieved the rms noise of 5μJy, only 20% higher than the theoretically expected level. In order to measure the polarization leakage (D-terms) we observed the unpolarized source 3C84. The polarization angle was calibrated using 3C48.

A radio spectral index image was produced by MS-MFS as well, and a post-deconvolution wide-band primary beam correction was applied to remove the effect of the frequency-dependent primary beam. This spectral index map was compared with a low-resolution spectral index map constructed within AIPS from primary-beam-corrected Stokes I images at each sub-band and smoothed to the resolution of the lowest sub-band. The results agreed, confirming that for this source, wide-band imaging via MS-MFS followed by a post-deconvolution primary beam correction was able to recover the same spectral information as traditional methods, but at a much improved angular resolution.

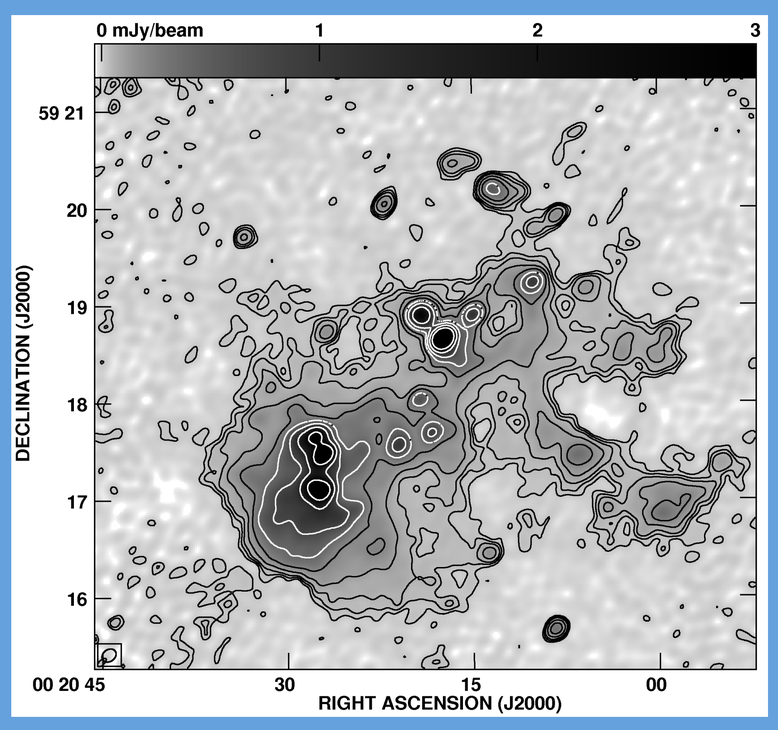

Figure 1. Total power radio continuum at 6 cm at 9.4" × 7.3" resolution as a quasi-logarithmic gray-scale image. Contours are at 3, 6, 10, 20, 40, 80, 150, 300 and 600 × 5 μJy/beam. The rms noise level is at 5 μJy/beam. The total power map is corrected for primary beam attenuation.

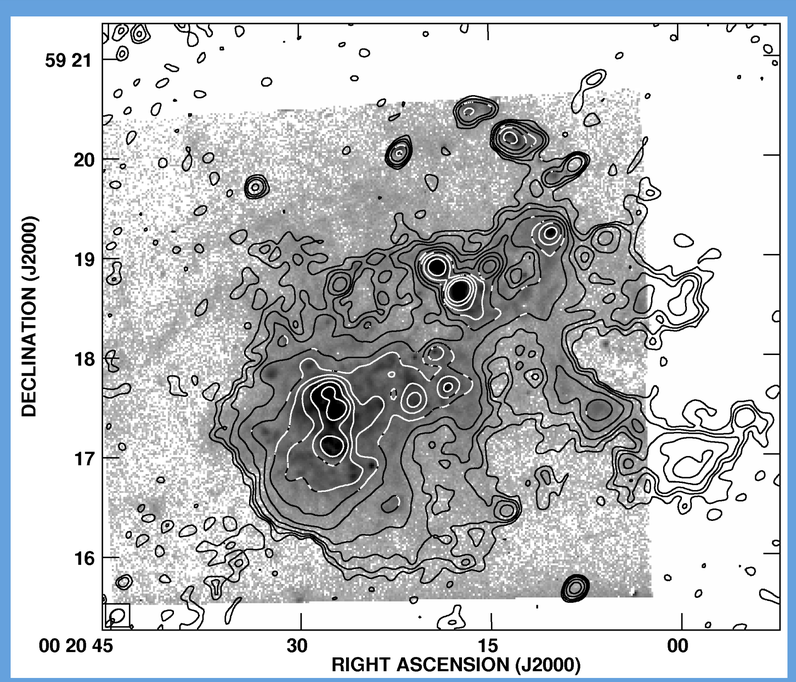

Figure 2. Same as Figure 1 but as an overlay on Ha shown as a quasi-logarithmic gray-scale image.

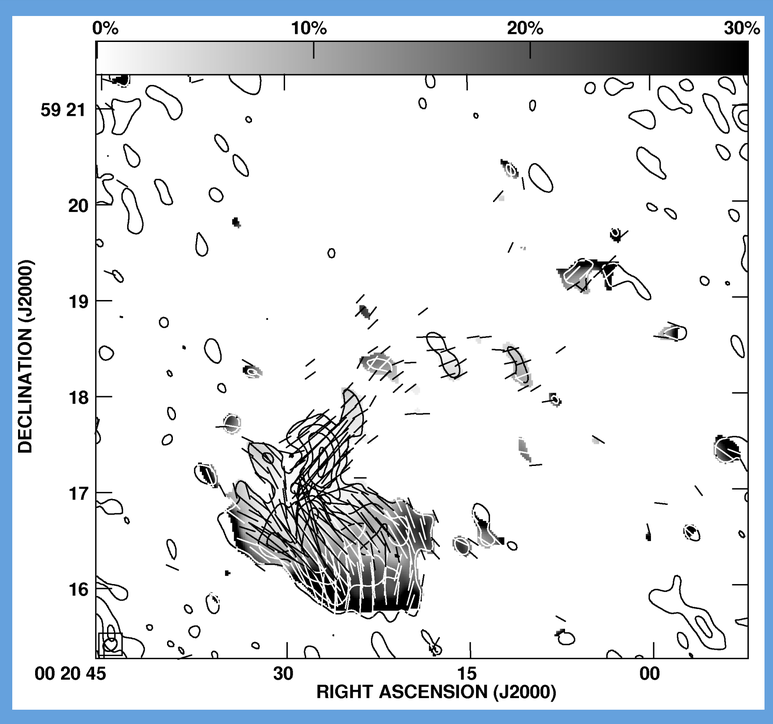

Figure 3. Polarized intensity and magnetic field orientation overlaid on the fractional polarization (gray scale) at 15" resolution. Polarized intensity contours are at 3, 6, 10, and 20 × 7 μJy/beam. The vector length is proportional to the polarized intensity, where 10" is equivalent to 22 μJy/beam (corrected for primary beam attenuation).

Results

Figure 1 shows our total power continuum radio map at 6 cm with a resolution of 9.4"×7.3". Contours start at 3 × the rms noise level and increase by a factor of about two with every further contour. We chose a logarithmic gray-scale to show the noise floor that is evenly distributed over the full extent of the map. To our knowledge this is the deepest radio continuum map of a dwarf galaxy yet made, going deeper than the preliminary VLA map, also at 6 cm, which reaches a noise of 9μJy (K. T. Chyzy 2011, private communication). The deep VLA map of NGC 1569 at 6 cm by Kepley et al. (2010, ApJ, 712, 536) has an rms noise of 8.5 μJy/beam but at a smaller beam size of ~4" and is much less sensitive to extended emission.

We compare in Figure 2 the radio continuum emission with a deep Ha map of Hunter & Elmegreen (2004, AJ, 128, 2170). The Ha is shown as a logarithmic gray-scale map to enhance weak emission features away from the main stellar body. The radio and Ha emission follow each other closely. The radio continuum peaks at the location of the Ha emission maxima that that trace HII complexes. Moreover, thanks to the exquisite dynamic range, we can compare the radio emission with extended Ha emission, including various shells and filaments. The large filament in the west with a length of 600 pc is the most prominent feature but we are sensitive enough to also detect the much weaker filaments in the eastern half.

The close correlation between the radio continuum and Ha emission suggests a large fraction of thermal radio emission from free-free emission. This is borne out by the radio spectral index map presented in Figure 4. The thermal emission has a radio spectral index of α = −0.1, whereas the non-thermal synchrotron emission has a spectral index of −0.7 (provided the cosmic-ray electrons are young, otherwise the spectrum is yet steeper). We find that almost all compact resolved sources within the galaxy have a flat spectral index between −0.1 and −0.2 indicative of a dominant thermal component. These are the compact HII regions with intense SF visible in Ha emission. We note that our radio spectral index map obtained via MS-MFS has a better resolution than that obtained with the conventional method, where the resolution is limited by the low-frequency map. This allows us to reliably identify the compact sources in the radio spectral index map that otherwise would be confused in the lower resolution version.

The map of the structure of the regular magnetic field is presented in Figure 3. We show the orientation of the large-scale magnetic field as measured from the linear polarization, where the length of the vectors is proportional to the polarized intensity. The degree of polarization in this region is 10%-20% indicating a significant ordered magnetic field component possibly enhanced by compression by the expanding superbubble. The magnetic field orientation is approximately NE-SW, where the polarized emission extends to the southern tip of the galaxy.

We also detect a magnetic field at the location of the two brightest HII regions in the southeastern part. At this position, away from the superbubble, the magnetic field orientation is more aligned with the stellar body. We cannot decide, based on the current data, if the magnetic field traverses the HII regions, because the field could also lie in front of or behind them, in a thick gas layer as is expected for dwarf galaxies. We note that the location of our polarized intensity and the orientation of the magnetic field agree well with that measured with the 100 m Effelsberg telescope (Chyzy et al. 2003, A&A, 405, 513), lending confidence to the performance of the EVLA and the CASA data reduction package.

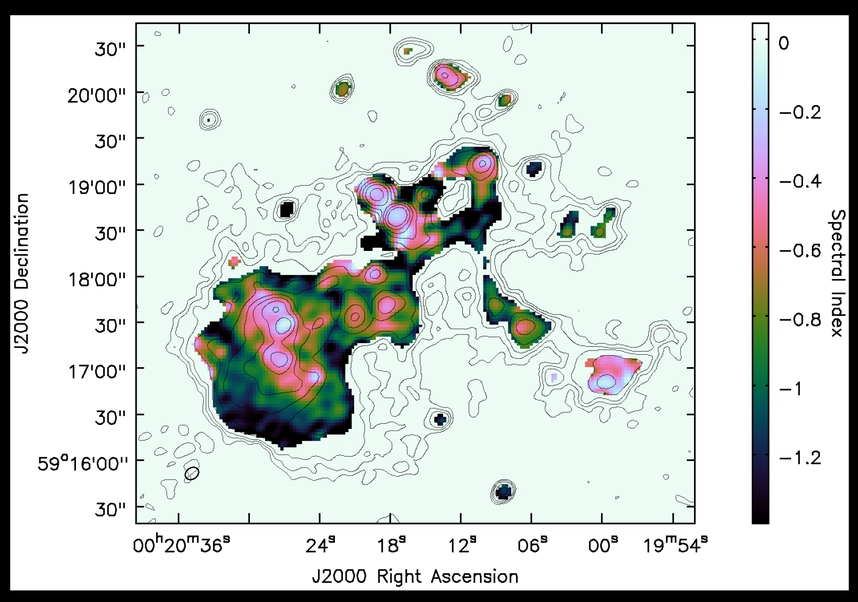

Figure 4. Radio spectral index map shown as a color-coded image at 9.4" × 7.3" resolution. The contours show the radio continuum emission and are similar to those in Figure 1. The frequency dependence of the primary beam was removed in a post-imaging step.

Discussion

We compared the flux densities of the radio emission and Ha emission averaged in 50 pc (10") boxes. The radio and Ha maps were convolved with a Gaussian to a half-power beam width of 50 pc prior to averaging. The result is presented in Figure 5. A power-law fit in the double logarithmic plot results in a power-law index of 0.97 ± 0.03 and is therefore consistent with a strictly linear relation between the two variables. The dashed line shows the relation if the radio flux density were purely thermal free-free emission calculated from the Ha flux density. The linear relation between the radio and the Ha brightness means that we can use both equally well as SF tracers. The SFR from the radio continuum is given by Condon (1992, ARA&A, 30, 575) and can be converted to an SFR density. If we convert the Ha emission into an SFR by the relation given in Kennicutt (1998, ARA&A, 36, 189), we can compare the two measurements. The radio SFR is a factor of three lower than that implied by Ha.

This means that IC 10 lies beneath the radio-SFR correlation and is radio dim. Further studies are required to investigate how this corresponds to the thermal and non-thermal fraction of the radio emission. In theory we expect that the high-frequency observations are a better tracer for the thermal component, especially since they require no correction for internal or foreground extinction. One goal of this project is to establish how well we can use radio emission as SF tracer even in such extreme cases as starburst dwarf galaxies.

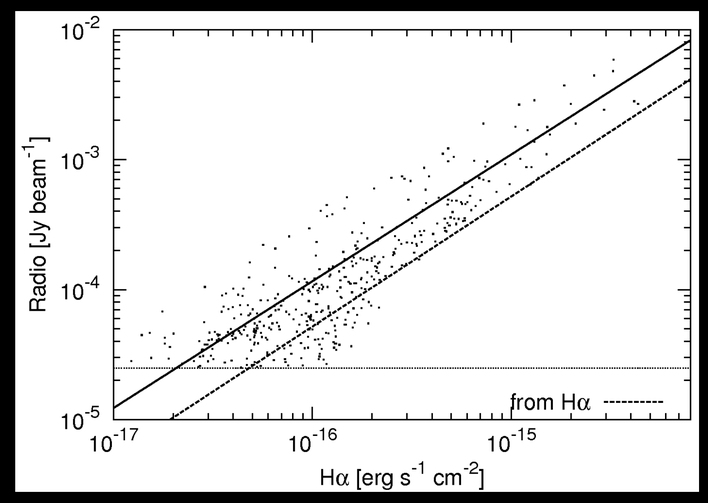

Figure 5. Comparison of the flux densities of the radio continuum emission at 6 cm with that of Ha at a scale of 50pc. The solid line shows a fit to the data as described in the text. The dashed line shows the expected contribution based on Ha to the radio continuum via thermal free-free emission (see the text for details). The horizontal line indicates 5 × the rms noise level in the radio map, where we clipped the radio data.